Containment and Consensus-based Distributed Coordination Control for Voltage Bound and Reactive Power Sharing in AC Microgrid

Han, Renke; Meng, Lexuan; Ferrari-Trecate, Giancarlo; Coelho, Ernane A. A.; Quintero, Juan Carlos Vasquez; Guerrero, Josep M.

Published in:
Proceedings of the 2017 IEEE Applied Power Electronics Conference and Exposition (APEC)

DOI (link to publication from Publisher):
10.1109/APEC.2017.7931207

Publication date:
2017

Document Version
Accepted author manuscript, peer reviewed version

Containment and Consensus-based Distributed Coordination Control for Voltage Bound and Reactive Power Sharing in AC Microgrid

Renke Han[1*], Lexuan Meng[1], Giancarlo F. Trecate[2], Ernane Antônio Alves Coelho[3], Juan C. Vasquez[1], Josep M. Guerrero[1]
[1] Department of Energy Technology, Aalborg University, Denmark
[2] Laboratoire d'Automatique, Ecole polytechnique fédérale de Lausanne, Switzerland
3 Universidade Federal de Uberlândia, Brazil
[*] rha@et.aau.dk

***Abstract*— This paper offers a highly flexible and reliable control strategy to achieve voltage bounded regulation and accurate reactive power sharing coordinately in AC Micro-Grids. A containment and consensus-based distributed coordination controller is proposed, by which each output voltage magnitude can be bounded within a reasonable range and the accurate reactive power sharing among distributed generators can be also achieved. Combined with the two proposed controllers and electrical part of the AC Micro-Grid, a small signal model is fully developed to analyze the sensitivity of different control parameters. The effectiveness of the proposed controller in case of load variation, communication failure, plug-and-play capability are verified by the experimental setup as an islanded Micro-Grid.**

Keywords*— Containment-based algorithm, voltage bound, small signal model, reactive power sharing, microgrid

I. INTRODUCTION

The Micro-Grid (MG) concept provides a promising mean of integrating large amounts of distributed generators (DG) into the power grid [1]. For islanded MGs, one of main challenges is to achieve the coordination control for accurate reactive power sharing and output voltage magnitudes regulation. *Q-V* droop control is applied to achieve reactive power sharing in a decentralized manner [2]. However, *Q-V* droop control is sensitive to the line impedance differences incurring inaccurate reactive power sharing, and voltage deviation is another problem. Furthermore, the coupling and tradeoff effects about reactive power sharing and voltage control are analyzed in details [3] based on the hierarchical control [4] [5].

In the hierarchical control architecture, centralized secondary controller can be used to achieve reactive power sharing and voltage restoration. Furthermore, an adaptive virtual impedance [6] is proposed to enhance the accuracy of reactive power sharing combined with centralized communication. Recently, it is realized that centralized controller suffers from high computational cost and low flexibility, while distributed control algorithms [7]-[9] are thus coming up to stage in MG applications [10]-[15]. A distributed method is proposed in [10] to achieve reactive power sharing through acquiring the average value of reactive power. However, each distributed controller need to know the output reactive power from all the other DGs with this approach. Based on the distributed leader-following tracking algorithm [8], paper [11] proposes a voltage tracking strategy by feedback linearization, achieving voltage magnitudes consensus. Meanwhile, a distributed finite-time control approach is used to achieve voltage and frequency restoration in finite time in [12] and [13]. However, the reactive power sharing problem is not considered by above voltage restoration controllers. An averaging-based method [8] has been applied in paper [14] to achieve reactive power sharing and keep the average value of voltage magnitudes equal to nominal value. In [15], a droop-free distributed method is proposed to achieve power sharing and fix average voltage value to nominal value, but the system cannot operate stable without droop control when all communication channels are failed down. Furthermore, fixed average voltage at nominal value is debatable under some conditions based on the standard [16]. Accordingly, most of the existing literatures focus on regulating the average value of output voltage magnitudes rather than bounding each output voltage magnitude in a flexible and reasonable range. Thus, a more flexible control strategy is required to bound all output voltage magnitudes into a reasonable range and achieve reactive power sharing.

To solve this challenge, the containment-based control [9] is considered as a reasonable and flexible approach, which can bound objects within a convex range maintaining the distributed fashion. In this paper, a fully distributed coordination control scheme including containment and consensus-based algorithm is proposed realizing a well coordination between reactive power sharing and voltage bound; Then, a small signal model considering proposed controllers is developed to analyze the system stability and provide control parameter design guide; Experimental results are shown to verify the controller performance, plug-and-play capability and resiliency to the communication failure.

II. CONTAINMENT AND CONSENSUS-BASED CONTROLLER FOR VOLTAGE BOUND AND REACTIVE POWER SHARING

This section explains the proposed distributed coordination control in details. A hierarchical control structure can be formulated to integrate of multiple functions seamlessly.

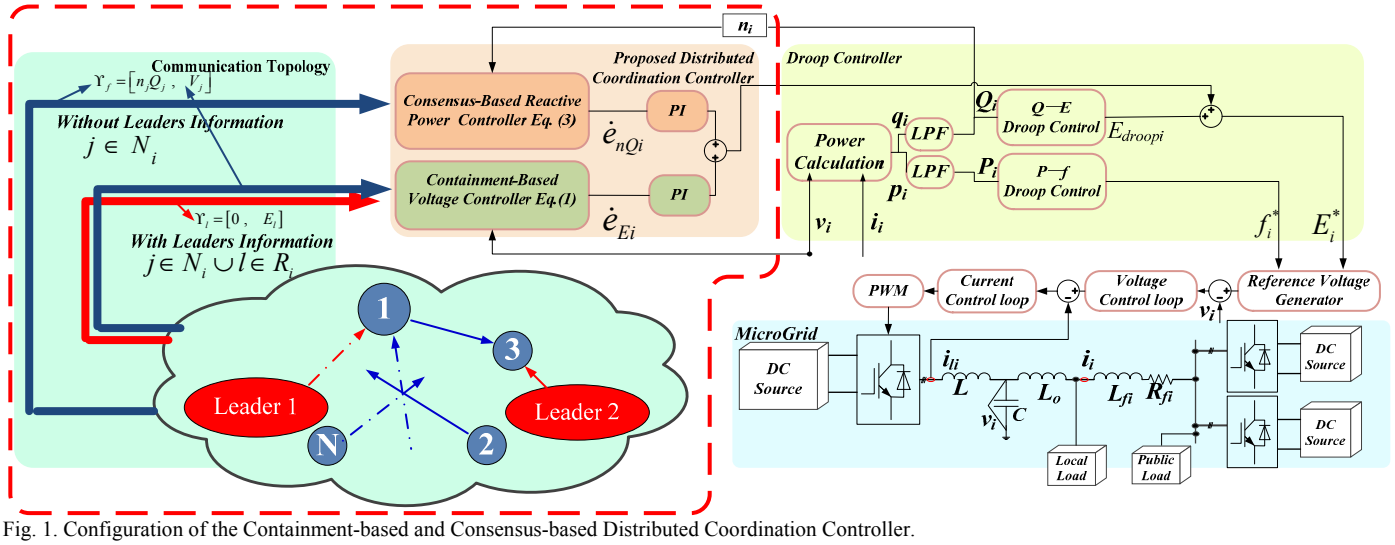

Fig. 1. Configuration of the Containment-based and Consensus-based Distributed Coordination Controller.

A. Definitions and Notations

For the control system with n distributed controllers, a controller is called a *leader* if it only provides information to its neighbors and does not receive information. A controller is called a *follower* if it can receive information from one or more neighbors through communication topology. Let N_i denote the set of i_{th}-controller neighbors chosen from followers, and R_i denote the set of leaders which can send its information to i_{th}-controller directly. The definition above is applied to containment-based voltage controller. Meanwhile, the consensus-based reactive power controller only uses the neighbors' information without the leaders' information.

Let C be a set in a real vector space $V \subseteq R^p$. The set C is called convex if, for any x and y in C, the point $(1-z)x+zy$ is also in C for any $z \in [0,1]$. The convex hull for a set of points $X=\{x_1,\ldots,x_q\}$ in V is the minimal convex set containing all points in X. Let $Co(X)$ denote the convex hull of X. When $V \subseteq R$, $Co(X)=\{x \mid x \in [\min x_i, \max x_i]\}$ which will be used in following. In addition, define vector $Z \in R^n$, then $diag(Z) \in R^{n\times n}$ as the diagonal matrix whose diagonal elements are the elements in vector Z. I_n is the unit matrix and 0_n is the zero $n \times n$ matrix.

For consensus-based controller, an adjacency matrix is defined as $A=[a_{ij}] \in R^{n\times n}$ with $a_{ij}=1$ if node i can receive information from node j otherwise $a_{ij}=0$; The Laplacian matrix is defined as $L_Q=[l_{ij}] \in R^{n\times n}$ with $l_{ii}=\sum_{j=1}^{n} a_{ij}$ and $l_{ij}=-a_{ij}$, $i \neq j$.

For containment-based controller, the range is formed by two leaders which are called the lower and upper voltage boundaries respectively. Another adjacency matrix is defined as $B=[b_{ij}] \in R^{n\times 2}$ with $b_{il}=1$ if node i can receive information from one of the two leaders otherwise $b_{il}=0$, in which l represents the label of two leaders; Another Laplacian matrix is defined as $L_E=[l_{ij}] \in R^{n\times(n+2)}$ with $l_{ii}=\sum_{j=1}^{n} a_{ij}+\sum_{l=n+1}^{n+2} b_{il}$ and for the last two rows of matrix L_E, all the element are zero because leaders do not receive information from others; for other rows, when $j<n$, $l_{ij}=-a_{ij}$, otherwise when $j>n$, $l_{ij}=-b_{ij}$.

B. Containment and Consensus-based Controller

The containment-based controller generates a correction term e_{Ei} for each DG to keep the voltage within a range which is a convex hull. The controller expression is defined as:

$$\dot{e}_{Ei}=-\sum_{j\in N_i} a_{ij}\left(E_{DGi}-E_{DGj}\right)-\sum_{l\in R_i} b_{il}\left(E_{DGi}-E_{bou}\right) \qquad (1)$$

where E_{DGi} and E_{DGj} are the voltage magnitudes of i-th DG and j-th DG respectively, E_{bou} is the voltage boundary which can be either upper boundary E_{Ubou} or lower boundary E_{Lbou}.

Eq. (1) can be written into matrix form as:

$$\dot{e}_E=-L_E\mathbf{E} \qquad (2)$$

where $E_{DG}=[E_{DG1}, \cdots E_{DGn}]^T$, $E_L=[E_{Ubou} \quad E_{Lbou}]^T$, $\mathbf{E}=[E_{DG}^T \quad E_L^T]^T$, $e_E=[e_{E1} \cdots e_{En}]^T$.

Then the error $\dot{e}_E$ is fed into a *PI* controller.

Consensus-based reactive power controller is defined as:

$$\dot{e}_{nQi}=-\sum_{j\in N_i} a_{ij}\left(n_iQ_i-n_jQ_j\right) \qquad (3)$$

where n_i and n_j are the reactive power droop gains, Q_i and Q_j are the output reactive for i-th DG and j-th DG.

(3) can be written into matrix form as:

$$\dot{e}_{nQ}=-L_QNQ \qquad (4)$$

where $N=diag\{[n_1, \cdots n_n]^T\}$, $e_{nQ}=[e_{nQ1} \cdots e_{nQn}]^T$.

Then the error $\dot{e}_{nQ}$ is fed into another *PI* controller.

To be mentioned, the proposed algorithm can be implemented in a module with specified input and output ports. For the containment-based voltage controller, each modular can be chosen as the leader of the system and for the consensus-based reactive power controller, each modular has the specified communication ports to receive the information from neighbors' information. The communication ports can be used by both the two proposed controllers.

The configuration of proposed controller is shown in Fig. 1 including the containment-based voltage controller and the consensus-based reactive power controller. The main contribution in this paper is included in the read dashed box. The information format from DGs (followers) is defined as $\Upsilon_{fj}=\left[n_jQ_j\ ,\ \ V_j\right]$, the information format from the leader is defined as $\Upsilon_l=\left[0\ ,\ \ E_{bou}\right]$.

III. Small Signal Stability Analysis

This section develops the small-signal model for stability analysis and parameters design for *n* DGs. The model includes proposed containment-based voltage controller, consensus-based reactive power controller, active and reactive power calculation, low-pass filter and droop control. It is assumed that the output voltage can follow the voltage reference very well by the inner loop and the inner loop regulation are not considered in this model. The whole model is based on the synchronous reference frame.

A. Small Signal Model for Proposed Controllers

For the containment-based voltage controller shown in (2), the small signal model is expressed as

$$\Delta\dot{e}_E=-L_E^{'}\Delta E_{DG} \tag{5}$$

where $L_E^{'}$ is the matrix which deletes the last two columns of matrix L_E neglecting the dynamic of leaders, $\Delta e_E=\left[\Delta e_{E1}\ \ \cdots\ \ \Delta e_{En}\right]^T$, $\Delta E_{DG}=\left[\Delta E_{DG1}\ \ \cdots\ \ \Delta E_{DGn}\right]^T$.

For the consensus-based reactive power controller in (4), the small signal model is expressed as

$$\Delta\dot{e}_{nQ}=-L_QN\Delta Q \tag{6}$$

where $\Delta e_{nQ}=\left[\Delta e_{nQ1}\ \ \cdots\ \ \Delta e_{nQn}\right]^T$, $\Delta Q=\left[\Delta Q_1\ \ \cdots\ \ \Delta Q_n\right]^T$.

Considering the dynamic voltage change, conventional *Q-V* droop controller can be rewritten (which is directly written into matrix form) as:

$$\dot{E}_{DG}=E^*-E_{DG}-NQ \tag{7}$$

in which a voltage disturb term $\dot{E}_{DG}$ is added.

As explained above, the two proposed controllers should provide control signals adding into (7) through PI controllers. Thus, the system can be written as:

$$\begin{aligned}\Delta\dot{E}_{DG}=&-\Delta E_{DG}-N\Delta Q-K_{pQ}L_QN\Delta Q-K_{pE}L_E^{'}\Delta E_{DG}\\&+K_{iQ}\Delta e_{nQ}+K_{iE}\Delta e_E\end{aligned} \tag{8}$$

where $K_{pQ}=diag\left(\left[k_{pQ1}\ \ \cdots\ \ k_{pQn}\right]^T\right)$ correspond to the proportional parameters and $K_{iQ}=diag\left(\left[k_{iQ1}\ \ \cdots\ \ k_{iQn}\right]^T\right)$ correspond to the integral parameters in PI controllers for the consensus-based reactive power controller, $K_{pE}=diag\left(\left[k_{pE1}\ \ \cdots\ \ k_{pEn}\right]^T\right)$ correspond to the proportional parameters and $K_{iE}=diag\left(\left[k_{iE1}\ \ \cdots\ \ k_{iEn}\right]^T\right)$ correspond to the integral parameters in PI controller for the containment-based voltage controller.

Due to the low-pass filter effect, the small signal model of output reactive power Q_i can be written as

$$\Delta\dot{Q}=-\omega_c\Delta Q+\omega_c\Delta q \tag{9}$$

where ω_c is the cut-off frequency of low-pass filter, the instant output reactive power is $\Delta q=\left[\Delta q_1\ \ \cdots\ \ \Delta q_n\right]^T$.

Considering synchronous reference frame for *i-th* DG, the vector voltage $\vec{E}_{DGi}$ can be written as

$$\vec{E}_{DGi}=E_{di}+jE_{qi} \tag{10}$$

where $E_{di}=E_{DGi}\cos\delta_i$, $E_{qi}=E_{DGi}\sin\delta_i$, $\delta_i=\arctan\left(E_{qi}/E_{di}\right)$

Linearizing the equation (10) of δ_i, we can get

$$\begin{aligned}\Delta\delta_i&=\left(\partial\delta_i/\partial E_{di}\right)\Delta E_{di}+\left(\partial\delta_i/\partial E_{qi}\right)\Delta E_{qi}\\&=m_{di}\Delta E_{di}+m_{qi}\Delta E_{qi}\end{aligned} \tag{11}$$

where $m_{di}=-E_{qi}/\left(E_{di}^2+E_{qi}^2\right)$, $m_{qi}=E_{di}/\left(E_{di}^2+E_{qi}^2\right)$.

Since $\Delta\omega_i(s)=s\Delta\delta_i(s)$, (13) can be rewritten as

$$\Delta\omega_i=m_{di}\Delta\dot{E}_{di}+m_{qi}\Delta\dot{E}_{qi} \tag{12}$$

Considering that $E_{DGi}=\left|\vec{E}_{DGi}\right|=\sqrt{E_{di}^2+E_{qi}^2}$, it can be linearized as

$$\Delta E_{DGi}=n_{di}\Delta E_{di}+n_{qi}\Delta E_{qi} \tag{13}$$

where $n_{di}=E_{di}/\sqrt{E_{di}^2+E_{qi}^2}$, $n_{qi}=E_{qi}/\sqrt{E_{di}^2+E_{qi}^2}$.

It follows that

$$\Delta\dot{E}_{DGi}=n_{di}\Delta\dot{E}_{di}+n_{qi}\Delta\dot{E}_{qi} \tag{14}$$

Thus, from the equation set consisted of (12), (14) for variables $\Delta\dot{E}_{di}$ and $\Delta\dot{E}_{qi}$, we have

$$\begin{cases}\Delta\dot{E}_{di}=m_{1i}\Delta\omega+m_{2i}\Delta\dot{E}_{DGi}\\ \Delta\dot{E}_{qi}=m_{3i}\Delta\omega+m_{4i}\Delta\dot{E}_{DGi}\end{cases}\tag{15}$$

where $m_{1i}=n_{qi}/\left(m_{di}n_{qi}-m_{qi}n_{di}\right)$, $m_{2i}=-m_{qi}/\left(m_{di}n_{qi}-m_{qi}n_{di}\right)$, $m_{3i}=n_{di}/\left(m_{qi}n_{di}-m_{di}n_{qi}\right)$, $m_{4i}=-m_{di}/\left(m_{qi}n_{di}-m_{di}n_{qi}\right)$.

Substituting the (8) and (13) into (15) and writing into matrix form as

$$\begin{cases}\Delta\dot{E}_d=M_1\Delta\omega+A_1N_d\Delta E_d+A_1N_q\Delta E_q\\ \qquad +A_2\Delta Q+M_2K_{iE}\Delta e_E+M_2K_{iQ}\Delta e_{nQ}\\ \Delta\dot{E}_q=M_3\Delta\omega+B_1N_d\Delta E_d+B_1N_q\Delta E_q\\ \qquad +B_2\Delta Q+M_4K_{iE}\Delta e_E+M_4K_{iQ}\Delta e_{nQ}\end{cases}\tag{16}$$

where $M_1=diag\left(\begin{bmatrix}m_{11} & \cdots & m_{1n}\end{bmatrix}^T\right)$,

$M_2=diag\left(\begin{bmatrix}m_{21} & \cdots & m_{2n}\end{bmatrix}^T\right)$, $M_3=diag\left(\begin{bmatrix}m_{31} & \cdots & m_{3n}\end{bmatrix}^T\right)$, $M_4=diag\left(\begin{bmatrix}m_{41} & \cdots & m_{4n}\end{bmatrix}^T\right)$, $N_d=diag\left(\begin{bmatrix}n_{d1} & \cdots & n_{dn}\end{bmatrix}^T\right)$, $N_q=diag\left(\begin{bmatrix}n_{q1} & \cdots & n_{qn}\end{bmatrix}^T\right)$, $A_1=-M_2\left(I_n+K_{pE}L_E^{'}\right)$, $A_2=-M_2\left(I_n+K_{pQ}L_Q\right)N$, $B_1=-M_4\left(I_n+K_{pE}L_E^{'}\right)$, $B_2=-M_4\left(I_n+K_{pQ}L_Q\right)N$, $\Delta E_d=\begin{bmatrix}\Delta E_{d1} & \cdots & \Delta E_{dn}\end{bmatrix}^T$, $\Delta E_q=\begin{bmatrix}\Delta E_{q1} & \cdots & \Delta E_{qn}\end{bmatrix}^T$, $\Delta\omega=\begin{bmatrix}\Delta\omega_1 & \cdots & \Delta\omega_n\end{bmatrix}^T$.

In addition, considering the active power droop control and the low power filter effect

$$\Delta\dot{\omega}=-\omega_c\Delta\omega-\omega_cM\Delta p\tag{17}$$

where $M=diag\left(\begin{bmatrix}m_1 & \cdots & m_n\end{bmatrix}^T\right)$ is the *P-f* droop gain, $\Delta p=\begin{bmatrix}\Delta p_i & \cdots & \Delta p_n\end{bmatrix}$ is the instant active power.

B. Small Signal Model for the Whole System

Considering load impedance and line impedance together, the conductance matrix *G* and susceptance matrix *B* can be written as

$$G=\begin{bmatrix}G_{11} & \cdots & G_{1n}\\ \vdots & \ddots & \vdots\\ G_{n1} & \cdots & G_{nn}\end{bmatrix},\ B=\begin{bmatrix}B_{11} & \cdots & B_{1n}\\ \vdots & \ddots & \vdots\\ B_{n1} & \cdots & B_{nn}\end{bmatrix}\tag{18}$$

Based on the *KCL* and *KVL* theorem, the small signal model between output current and voltage can be written as

$$\begin{cases}\Delta I_d=G\Delta E_d+(-B)\Delta E_q\\ \Delta I_q=B\Delta E_q+G\Delta E_d\end{cases}\tag{19}$$

where $\Delta I_d=\begin{bmatrix}\Delta I_{d1} & \cdots & \Delta I_{dn}\end{bmatrix}^T$, $\Delta I_q=\begin{bmatrix}\Delta I_{q1} & \cdots & \Delta I_{qn}\end{bmatrix}^T$.

Since instant active and reactive power are obtained through an orthogonal system as

$$\begin{cases}p_i=3/2\left(E_{di}I_{di}+E_{qi}I_{qi}\right)\\ q_i=3/2\left(E_{qi}I_{di}-E_{di}I_{qi}\right)\end{cases}\tag{20}$$

The small signal model of the instant output power is presented as

$$\begin{cases}\Delta p=3/2\left(I_d\Delta E_d+I_q\Delta E_d+E_d\Delta I_d+E_q\Delta I_q\right)\\ \Delta q=3/2\left(-I_q\Delta E_d+I_d\Delta E_d+E_q\Delta I_d-E_d\Delta I_q\right)\end{cases}\tag{21}$$

where $I_d=diag\left(\begin{bmatrix}I_{d1} & \cdots & I_{dn}\end{bmatrix}^T\right)$, $I_q=diag\left(\begin{bmatrix}I_{q1} & \cdots & I_{qn}\end{bmatrix}^T\right)$, $E_d=diag\left(\begin{bmatrix}E_{d1} & \cdots & E_{dn}\end{bmatrix}^T\right)$, $E_q=diag\left(\begin{bmatrix}E_{q1} & \cdots & E_{qn}\end{bmatrix}^T\right)$.

Combining with (19), (21), the small signal model of instant active and reactive power can be expressed as

$$\begin{cases}\Delta p=S_1\Delta E_d+S_2\Delta E_q\\ \Delta q=S_3\Delta E_d+S_4\Delta E_q\end{cases}\tag{22}$$

where $S_1=3/2\left(I_d+E_dG+E_qB\right)$, $S_2=3/2\left(I_q-E_dB+E_qG\right)$, $S_3=3/2\left(-I_q+E_qG-E_dB\right)$, $S_4=3/2\left(I_d-E_qB-E_dG\right)$.

Substituting (22) into (9), (17) and Substituting (13) into (5) and combining (6), (16), we can obtain the whole system model as

$$\dot{X}=FX\tag{23}$$

where

$$F=\begin{bmatrix}-\omega_cI_n & -\omega_cMS_1 & -\omega_cMS_1 & 0_n & 0_n & 0_n\\ M_1 & A_1N_d & A_1N_q & A_2 & M_2K_{iE} & M_2K_{iQ}\\ M_3 & B_1N_d & B_1N_q & B_2 & M_4K_{iE} & M_4K_{iQ}\\ 0_n & \omega_cS_3 & \omega_cS_4 & -\omega_cI_n & 0_n & 0_n\\ 0_n & -L_E^{'}N_d & -L_E^{'}N_q & 0_n & 0_n & 0_n\\ 0_n & 0_n & 0_n & -LQ_N & 0_n & 0_n\end{bmatrix},$$

$$X=\begin{bmatrix}\Delta\omega^T & \Delta E_d^T & \Delta E_q^T & \Delta Q^T & \Delta e_E^T & \Delta e_{nQ}^T\end{bmatrix}^T.$$

C. Stability Analysis

To analyze the model quantitatively, a MG including four parallel connected DGs, loads are considered as a study case. Root locus plots are shown in *S-domain* to reflect the dynamic behavior of the system considering different control parameters. The model can be extended to *N* DGs to analyze the system stability.

Fig. 2 shows root locus considering the proportional coefficient K_{pE} of *PI* controller for containment-based controller changed from 7 to 15. From the enlarged part in Fig. 2, it is shown that two dominating poles near the imaginary axis are moving towards the real axis and away from the imaginary axis which indicate that the system is becoming more and more damped. Six complex poles which are also affected by K_{pE}, are moving away from the imaginary axis, thus improving the response speed.

Fig. 3 shows root locus considering integral coefficient K_{iE} of *PI* controller for containment-based controller changed from 1 to 100. From the enlarged part in Fig. 3, it is shown that two dominating poles are moving away from real axis, which means the system is becoming less damped. Meanwhile, two poles on the real axis are moving away from original point. Six complex poles are less affected than that of proportional coefficient K_{pE}.

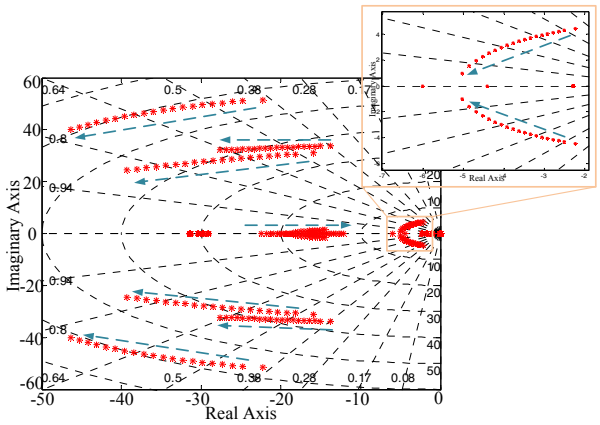

Fig. 2. Root locus plot $7<K_{pE}<15$.

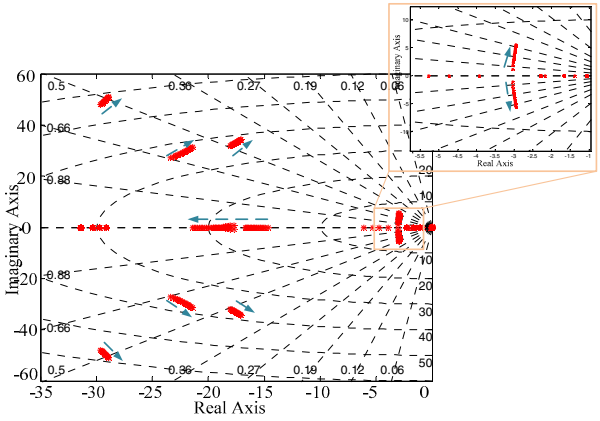

Fig. 3. Root locus plot $1<K_{iE}<100$

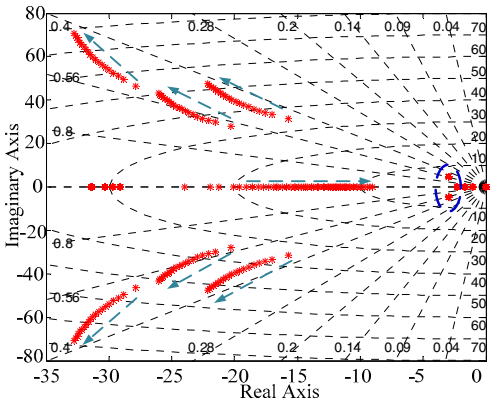

Fig. 4. Root locus $7<K_{pQ}<15$;

Fig. 4 shows root locus considering proportional coefficients K_{pQ} for a *PI* controller for consensus-based controller changed from 7 to 15. It can be observed that two dominating poles in the blue circle are almost not affected. In addition, one pole on the real axis moves towards origin point which can slow down the response speed. Six complex poles are moving away from real axis, which means the system is becoming less damped.

Fig. 5 shows root locus considering integral coefficients K_{iQ} of *PI* controller for consensus-based control changed from 30 to 120. The two dominating poles in the blue circle are also not affected. One dominating pole on the real axis is moving away from the original point which can increase the system response speed. Six complex poles are moving towards the imaginary axis which makes the system be less damped.

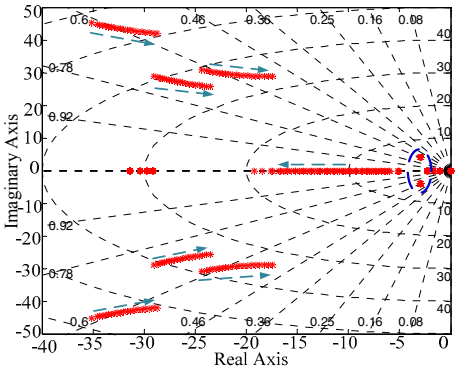

Fig. 5. Root locus plot $30<K_{iQ}<120$.

Fig. 6 (a) shows that the eigenvalues are not affected by only changing the inductive load and Fig. 6 (b) shows that the eigenvalues are not affected by only changing the resistive load. It indicates that the robustness of the system is very well and not affected by the load changes.

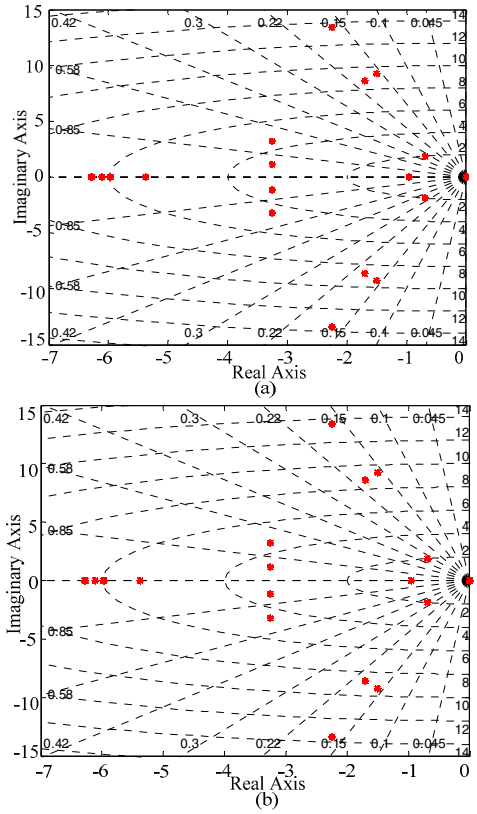

Fig. 6. Root locus: (a) Inductive Load Change from *0.01 H* to *1 H*; (b) Resistive Load Change from *15Ω* to *1500Ω*.

IV. EXPERIMENTAL RESULTS

The proposed control scheme is implemented and tested in an experimental MG setup operated in islanded mode shown in Fig. 7 at the AAU-Microgrid Research Laboratory. The setup consists of four parallel-configured power electronics inverters, a real-time control and monitoring platform, LCL filters and RL loads. Communication link is only built between neighboring units shown in the top left corner of Fig. 7. Rated active and reactive power has the ratio 2: 2: 1: 1 for DG_1-DG_4. The nominal voltage magnitude is set to 325 V with 1% voltage boundary $(325*(1\pm1\%))$.

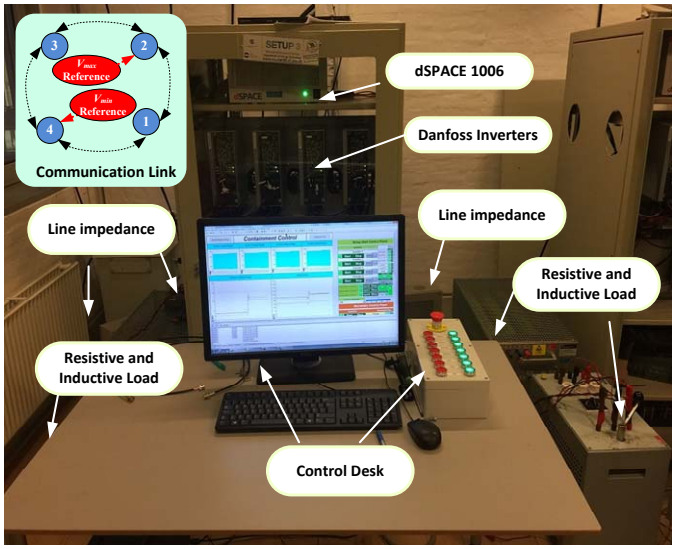

Fig. 7. Experimental setup in AAU-Microgrid research laboratory

A. Case 1: Performance Assessment and Comparison

Fig. 8 shows the performance of the proposed controller. Fig. 8 (a) shows the voltage performance and Fig. 8 (b) shows the performance of reactive power sharing. Before t=*T1*, the system is controlled by the conventional droop control. The voltage magnitude drops are obvious and the reactive power sharing are inaccurate. At t=*T1*, the proposed controller is activated. Then, the output voltage can be bounded within prescribed boundary and the reactive power are sharing proportionally.

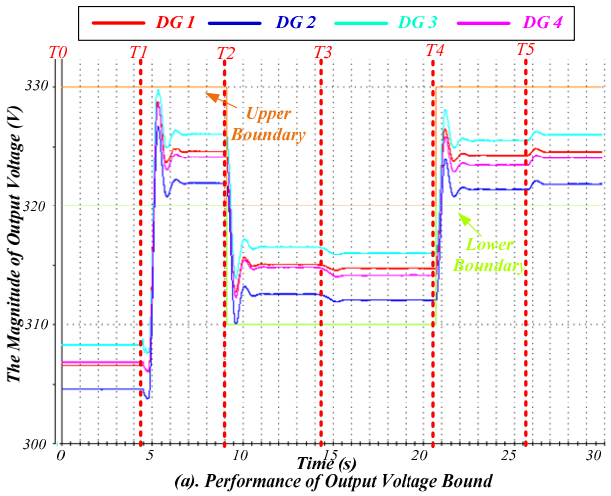

(a). Performance of Output Voltage Bound

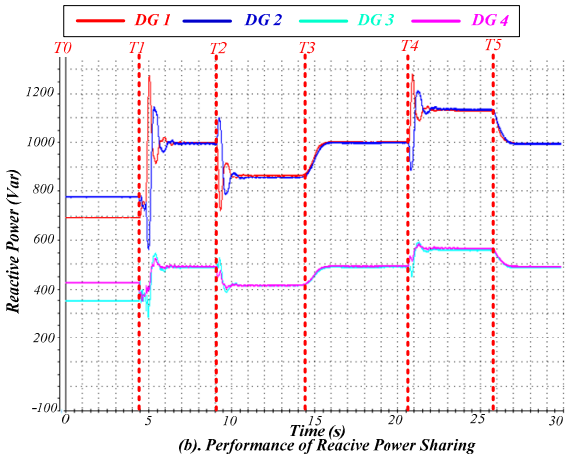

(b). Performance of Reacive Power Sharing

Fig. 8. Performance evaluation of the proposed controller

Furthermore, between t=*T2* and t=*T4*, the boundary is changed and the output voltage magnitudes are followed the changed boundary into the new range. Meanwhile, the performance of reactive power sharing can also be guaranteed. In addition, at t=*T3*, the load is changed and the reactive power sharing is also very well. After t=*T4*, the voltage boundary is restored and both the voltage and reactive power sharing performance are kept well. It is shown that after activating the proposed controller, the output voltage magnitudes are bounded within the dynamic range. Meanwhile the output reactive power can be proportional shared during the whole process.

B. Case 2: Communication Failure Resiliency

Resiliency to a single communication link failure is studied in Fig. 9. The communication link between DG_2 and DG_3 has been disabled at =*T6*. As shown in the enlarged part of Fig. 9 (a) and (b), after small oscillations, it does not have any impact on the performance of voltage bound and reactive power sharing. After that, the load is increased and decreased at t=*T7* and *T8* respectively. The dynamic response is a little slower than the condition without communication failure. The steady-state control performance is unaffected. It is concluded that the steady-state performance of the proposed controller cannot be affected by a single communication link failure so long as the communication network remains connected from the perspective of graph theory.

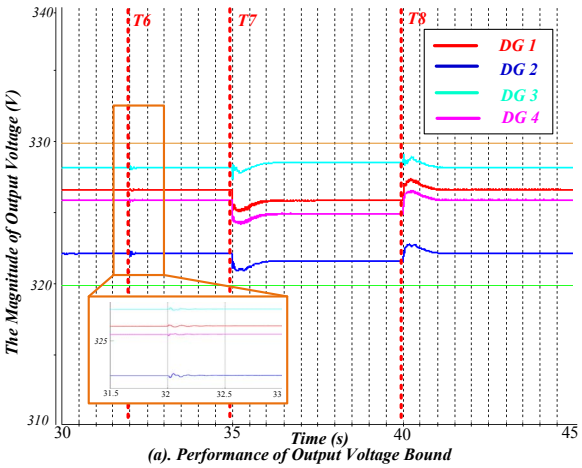

(a). Performance of Output Voltage Bound

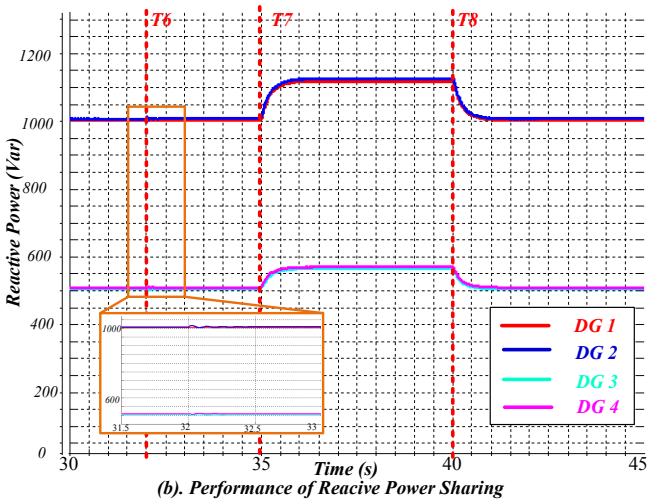

Fig. 9. Resiliency to a Single Communication Failure Between DG_2 and DG_3

C. Case 3: Plug-and-Play Study

This case studies the plug-and-play capability of the proposed controller. DG_4 is unplugged at t=*T9*. Thus, the output voltage and reactive power from DG_4 decay to zero as shown in Fig. 10 (a). To be noted, a source failure also means loss of communication links connected to other sources. Meanwhile, the performance from other three DGs can be kept very well by the proposed controller as shown in Fig. 10.

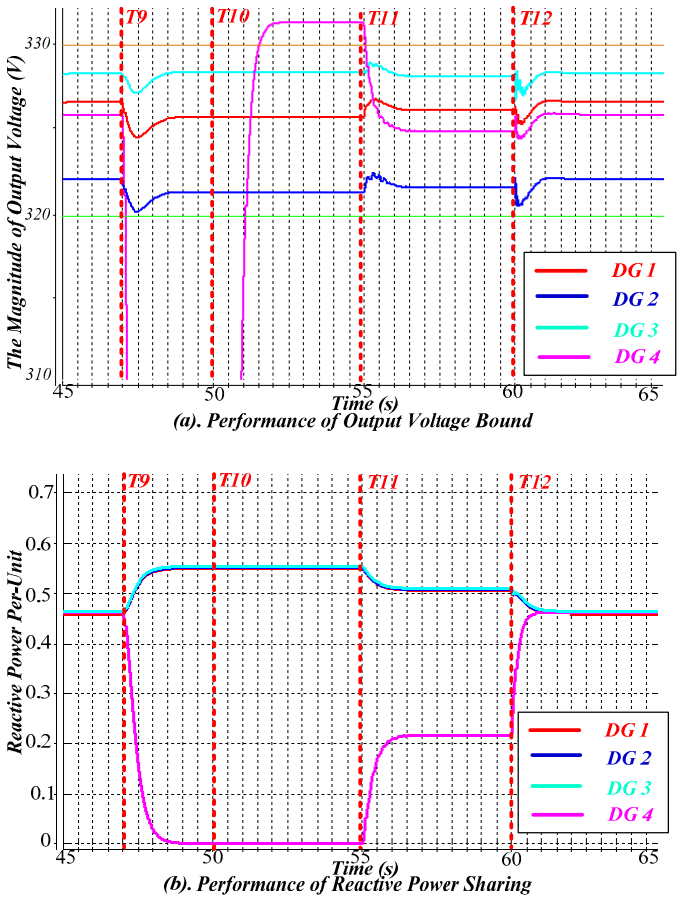

Fig. 10. Plug-and Play Study for DG 4

To illustrate, Fig. 10 (b) shows the per-unit value of output reactive power to decrease the range of *y*-axis. At t=*T10*, DG_4 begin to synchronize the frequency with the system. After successful synchronization, at t=*T11*, DG_4 is plugged back without activating the proposed controller. At t=*T12*, the proposed controller and communication are activated for DG_4. It can be verified that both the performances about voltage bound and reactive power sharing are readjusted excellent among four DGs after activating the proposed controller for DG_4.

V. Conclusion

A fully distributed coordination controller including both containment-based and consensus-based controllers is proposed to offer a highly flexible and reliable operation of DGs, achieving the voltage magnitudes bound within a reasonable range and accurate reactive power sharing. A detailed small signal model is derived and the effects of different parameters change for the proposed controller are analyzed. Experimental results are presented to demonstrate the effectiveness of proposed controller including performance assessment and comparison, resiliency for communication failure and plug and play study.

References

[1] DOE Microgrid Workshop Report, U.S. Dept. Energy, San Diego, CA, USA, Aug. 2011.

[2] M. C. Chandorkar, D. M. Divan, and R. Adapa, "Control of parallel connected inverters in standalone AC supply systems," *IEEE Trans. Ind. Appl*., vol. 29, no. 1, pp. 136-143, Jan./Feb. 1993.

[3] R. Han, L. Meng, J. M. Guerrero, Q. Sun, J. C. Vasquez, "Coupling/Tradeoff Analysis and Novel Containment Control for Reactive Power, Output Voltage in Islanded Micro-Grid," *in Industrial Electronics, IECON 42th Annual Conference of IEEE*, 2016.

[4] J. M. Guerrero, J. C. Vasquez, J. Matas, M. Castilla, L. G. D. Vicuna, and M. Castilla, "Hierarchical control of droop-controlled ac and dc microgrids—A general approach toward standardization," *IEEE Trans. Ind. Electron*., vol. 58, no. 1, pp. 158-172, Jan. 2011.

[5] L. Meng, A. Luna, E. Diaz, B. Sun, T. Dragicevic, M. Savaghebi, J. Vasquez, J. Guerrero, M. Graells, "Flexible System Integration and Advanced Hierarchical Control Architectures in the Microgrid Research Laboratory of Aalborg University," *IEEE Trans. Industry Applications*, vol. 52, no. 2, pp.1736-1749, Mar/Apr. 2016.

[6] H. Mahmood, D. Michaelson, J. Jiang, "Accurate reactive power sharing in an islanded microgrid using adaptive virtual impedances," *IEEE Trans. on Power Electron.*, vol. 30, no. 3, pp. 1605-1617, Mar. 2015.

[7] A. Jadbabaie, J. Lin, and A. S. Morse, "Coordination of groups of mobile autonomous agents using nearest neighbor rules," *IEEE Trans. Autom. Control,* vol. 48, no. 6, pp. 988–1001, Jun. 2003.

[8] R. Olfati-Saber, J. A. Fax, and R. M. Murray, "Consensus and cooperation in networked multi-agent systems," *Proc. IEEE*, vol. 95, no. 1. Pp. 215-233, Jan. 2007.

[9] M. Ji, G. Ferrari-Trecate, M. Egerstedt, and A. Buffa, "Containment control in mobile networks," *IEEE Trans. on Autom. Control*, vol. 53, no. 8, pp. 1972–1975, Sep. 2008.

[10] S. Qobad, J. M. Guerrero, J. C. Vasquez , "Distributed Secondary Control for Islanded MicroGrids - A Novel Approach," *IEEE Trans. on Power Electron.*, vol. 29, no. 2, pp. 1018-1031, Feb. 2014.

[11] A. Bidram, A. Davoudi, F. L. Lewis, and J. M. Guerrero, "Distributed cooperative secondary control of microgrids using feedback linearization," *IEEE Trans. Power Syst*., vol. 28, no. 3, pp. 3462–3470, Aug. 2013.

[12] F. Guo, C. Wen, J. Mao, and Y.-D. Song, "Distributed secondary voltage and frequency restoration control of droop-controlled inverter-

based microgrids," *IEEE Trans. Ind. Electron.,* vol. 62, no. 7, pp. 4355–4364, Jul. 2015.

[13] S. Zuo; A. Davoudi; Y. Song; F. L. Lewis, "Distributed Finite-time Voltage and Frequency Restoration in Islanded AC Microgrids, " *IEEE Trans. Ind. Electron.*, vol. 63, no. 10, pp. 5988-5997, Oct. 2016.

[14] J. W. Simpson-Porco, Q. Shafiee, F. Dorfler, J. C. Vasquez, J. M. Guerrero, F. Bullo, "Secondary Frequency and Voltage Control of Islanded Microgrids via Distributed Averaging," *IEEE Trans. Ind. Electron*., vol. 58, no. 1, pp. 7025-7038, Nov. 2016.

[15] V. Nasirian, Q. Shafiee, J. M. Guerrero, F. L. Lewis, A. Davoudi, "Droop-free distributed control for AC microgrid, " *IEEE Trans. on Power Electron*., vol. 31, no. 2, pp. 1600-1617, Feb. 2016.

[16] "Technical paper—Definition of a set of requirement to generating units," in UCTE, 2008.